Russian Journal of Physiology – Heart and Circulatory Physiology **280: H2053-H2060, 2001; 0363-6135/01**
Vol. 280, Issue 5, December 2002

Effect of various diets prescribed in The Indian System of Medicine on the resting potential of cells.

DR. Ravishankar Polisetty and Dr. Nikolskiy Peter Vladislavovich.
The Bakulev Centre for Cardiac Surgery, Russian Medical Academy, Moscow, Russian Federation.

ABSTRACT

Our work is primarily to prove that cells of the same tissue would exist with different resting potentials depending on the dietary intake as prescribed in the Indian system of Medicine. We had used the action potentials in the heart muscle as a reference parameter for this purpose. We had used three groups, each group containing 15 in numbers, of Male Wistar rats, which were respectively fed with diets as prescribed for increasing Vata, Pitta and Kapha explained in the Indian system of medicine. We used two control group of rats. All the five groups were fed with balanced diet for a period of three weeks. One group of control rats was sacrificed and we measured action potentials from the intact heart. The action potentials showed an average resting potential of about – 84.5 mV. The second control group of rats was continued with the same diet. The three experimental rats were then fed with vata, pitta and kapha enhancing diets. At the end of another three weeks all the rats in all groups were sacrificed and action potentials were measured from their intact hearts. Intracellular calcium handling plays an important role in cardiac electrophysiology. Using two fluorescent indicators, we developed an optical mapping system that is capable of measuring calcium transients and action potentials at 256 recording sites simultaneously from the intact rat heart. On the basis of in vitro measurements of dye excitation and emission spectra, excitation and emission filters at 515 ± 5 and >695 nm, respectively, were used to measure action potentials with di-4-ANEPPS, and excitation and emission filters at 365 ± 25 and 485 ± 5 nm, respectively, were used to measure calcium transients with indo 1. The percent error due to spectral overlap was small when action potentials were measured (1.7 ± 1.0%, $n = 3$) and negligible when calcium transients were measured (0%, $n = 3$). Recordings of calcium transients, action potentials, and isochrone maps of depolarization time and the time of calcium transient onset indicated negligible error due to fluorescence emission overlap. These data demonstrate that the error due to spectral overlap of indo 1 and di-4-ANEPPS is sufficiently small, such that optical mapping techniques can be used to measure calcium transients and action potentials simultaneously in the intact heart. The values of Action potentials in the second control group did not vary much with those in the first control group. The values of Action potentials in the vata food fed rats where very close to the resting potential. Those, fed with Pitta enhancing diet varied between -86.5mV and -93.5mV. Anil those fed with Kapha enhancing diet had varied between -105.28mV and -112.28mV. These findings in our view are very important to classify cells based on their resting potentials. The findings prove that the more the resting potential, the lesser the external stimulus needed to excite and generate an Action potential which gives a greater understanding of arrhythmias in cardiac muscles and various nervous and other disorders.

intracellular calcium; electrophysiology; optical mapping; di-4-ANEPPS; indo 1, Vata, Pitta, Kapha

INTRODUCTION

INTRACELLULAR CALCIUM is an important ion that has many direct effects on the electrophysiology of the heart. For example, the effects of intracellular calcium on membrane calcium channels, nonselective cation channels, and exchangers can significantly influence transmembrane potential (2). Furthermore, there is considerable evidence that abnormal intracellular calcium handling plays an important role in arrhythmias associated with electrical alternans (17) and heart failure (29, 37) and during the initiation of ventricular fibrillation (26). More recently, data from isolated myocytes suggest regional heterogeneities of intracellular calcium handling associated with heart failure (15, 24). Therefore, to better understand the mechanistic relationship between intracellular calcium handling and arrhythmogenesis, in various diets, a method for mapping calcium transients and action potentials simultaneously from the intact heart is essential.

Fluorescent indicators of intracellular calcium (12) have been used extensively to measure calcium transients and absolute intracellular calcium at the level of the intact heart (3, 16, 21) and single cell (1). Likewise, voltage-sensitive fluorescent indicators have been used to map action potentials from the intact heart (27) and have been used extensively to study cellular mechanisms of arrhythmias (10, 11, 38). Because the excitation and emission wavelengths of fluorescent indicators vary from ultraviolet to near infrared, it is possible to measure more than one cellular parameter by using multiple indicators. To do so, the spectral overlap must be minimal, such that fluorescence of one indicator does not significantly overlap with that of the other. We developed an optical mapping system to measure with high resolution intracellular calcium transients and action potentials simultaneously from the intact heart. We demonstrate that there is negligible error caused by spectral overlap of indo 1 and di-4-ANEPPS and that optical mapping techniques can be used to measure calcium transients and action potentials simultaneously with high resolution.

METHODS

Experiments were carried out in accordance with RF (Russian Federation) Public Health Service (under the Ministry of Health and Social Dvelopment) guidelines for the care and use of laboratory animals. Male wistar rats (n = 15, 120 – 150g) in the first control group were fed with balanced diet as prescribed by the Ethical committee of the Moscow State University for about three weeks and then were anesthetized with pentobarbital sodium (30 mg/kg ip), and their hearts were rapidly excised and perfused by an aortic cannula as Langendorff preparations with oxygenated (95% O_2-5% CO_2) Tyrode solution containing (mM) 121.7 NaCl, 25.0 $NaHCO_3$, 2.74 $MgSO_4$, 4.81 KCl, 5.0 dextrose, and 2.5 $CaCl_2$ (pH 7.40, 32°C). Perfusion pressure was maintained at 60-70 mmHg by regulating coronary perfusion flow with a digital dual-head roller pump. Hearts were stained by direct coronary perfusion for ~10 min with the voltage-sensitive indicator di-4-ANEPPS

(Molecular Probes, Eugene, OR) dissolved in 0.19 ml of ethanol at a final concentration of 15 μM and for ~30 min with the calcium-sensitive indicator indo 1-AM (Molecular Probes) dissolved in a 0.5-ml solution of DMSO and Pluronic (20% wt/vol) at a final concentration of 5 μM. In all experiments, 2,3-butanedione monoxime (10 mM) was used to ensure that motion artifact, if present, did not influence our results.

Perfused hearts were placed in a custom-built Plexiglas chamber that was attached to a micromanipulator (18). The mapping field was positioned over the left anterior descending coronary artery, just below its bifurcation with the diagonal coronary artery. The anterior surface of the heart was stabilized with a movable piston against an imaging window. To avoid epicardial surface cooling and temperature gradients, the heart was immersed in the coronary effluent, which was maintained at a constant temperature equal to the perfusion temperature with a heat exchanger located in the chamber. The electrocardiogram (ECG) was monitored using three silver disk electrodes fixed to the chamber in positions roughly corresponding to ECG limb leads I, II, and III. ECG signals were filtered (0.3-300 Hz), amplified (×1,000), and displayed on an oscilloscope. To ensure physiological stability of the preparation, the ECG, coronary pressure, coronary flow, and perfusion temperature were monitored continuously throughout each experiment. Preparations remained viable for 3-4 h, but the experimental protocols typically lasted <1 h.

Spectrofluorometer Measurements

To select optical filters for measuring transmembrane potential and intracellular calcium simultaneously, in vitro excitation and emission spectra of indo 1 and di-4-ANEPPS were obtained with a spectrofluorometer. In four experiments, hearts were stained with indo 1 (n = 2) or di-4-ANEPPS (n = 2). Immediately after they were stained with indo 1, hearts were perfused with a zero-calcium Tyrode solution to measure the peak emission of unbound indo 1. This peak was chosen, because unbound indo 1 is more efficiently excited at 365 nm and is closer to the emission spectrum of di-4-ANEPPS than is the bound form of indo 1. For all hearts, a portion of the left ventricle was dissected and placed in an ultraviolet-grade cuvette with the epicardial surface at a 45° angle with respect to the surface of the cuvette to maximize fluorescence detection. The cuvette was then placed in the sample compartment of a spectrofluorometer (SLM Aminco 8100, Spectronic Instruments, Rochester, NY) maintained at a constant temperature of 32°C. Excitation and emission scans were completed within 5 min.

Optical Mapping System

We have developed an optical mapping system that is capable of measuring high-fidelity fluorescent signals with high spatial and temporal resolution simultaneously at 256 recording sites from the intact heart (Fig. 1). Action potentials were measured using di-4-ANEPPS with filtered excitation light (515 ± 5 nm; Omega Optical, Brattleboro, VT) obtained from a 180-W quartz tungsten halogen lamp light source (Oriel, Stratford, CT) directed to the heart with a liquid light guide. Calcium transients were measured using indo 1 with filtered excitation light (365 ± 25 nm; Omega Optical) obtained from a 250-W mercury arc lamp light source (Oriel) directed to the heart with a second liquid light guide. Excitation light from both light guides was directed to the same location on

the heart. Fluoresced light from the heart was collected by a tandem lens assembly (22, 30) as shown in Fig. 1. The tandem lens assembly consisted of four high-numerical aperature complex photographic lenses (85 mm F/1.4, 35 mm F/1.4, 105 mm F/2.0, and 105 mm F/2.0; Nikon, Tokyo, Japan) placed facing each other. A dichroic mirror (560 nm; Omega Optical) placed between the lenses passes light of longer wavelengths to an emission filter (>695 nm; Shott Glass Technologies, Duryea, PA) and a 16 × 16 element photodiode array (*detector 1*) and reflects light of shorter wavelengths to a second emission filter (485 ± 5 nm; Chroma, Brattleboro, VT) and a 16 × 16 element photodiode array (*detector 2*). Emission wavelengths were chosen on the basis of the excitation and emission spectra obtained using the spectrofluorometer (see RESULTS). All optical components of the tandem lens system (e.g., lenses, filter holders, detectors) were aligned and rigidly mounted to optical rails. Before each experiment, optical alignment was verified with an accuracy of ~35 μm by directing an image of *detectors 1* and *2* onto the charge coupled device videocamera (Pulnix, Sunnyvale, CA) for display on a video monitor. Photocurrent from all 256 photodiodes of each detector array was passed through low-noise current to voltage converters (Hamamatsu, Hamamatsu City, Japan) and then underwent postamplification (×1, ×50, ×200, ×1,000) with AC coupling (10-s time constant), followed by low-pass antialias filtering (500 Hz). Signals recorded from each photodiode and ECG signals were multiplexed and digitized with 12-bit precision at a sampling rate of 1,000 Hz/channel (Microstar Laboratories, Bellevue, WA). For the present study, an optical magnification of ×1.24 resulted in a total mapping field of 1.4 × 1.4 cm with 0.09 cm of spatial resolution. To view, digitize, and store the position of the mapping array relative to anatomic features, a mirror was temporarily inserted between the lenses of the tandem lens assembly to direct reflected light to the charge coupled device videocamera.

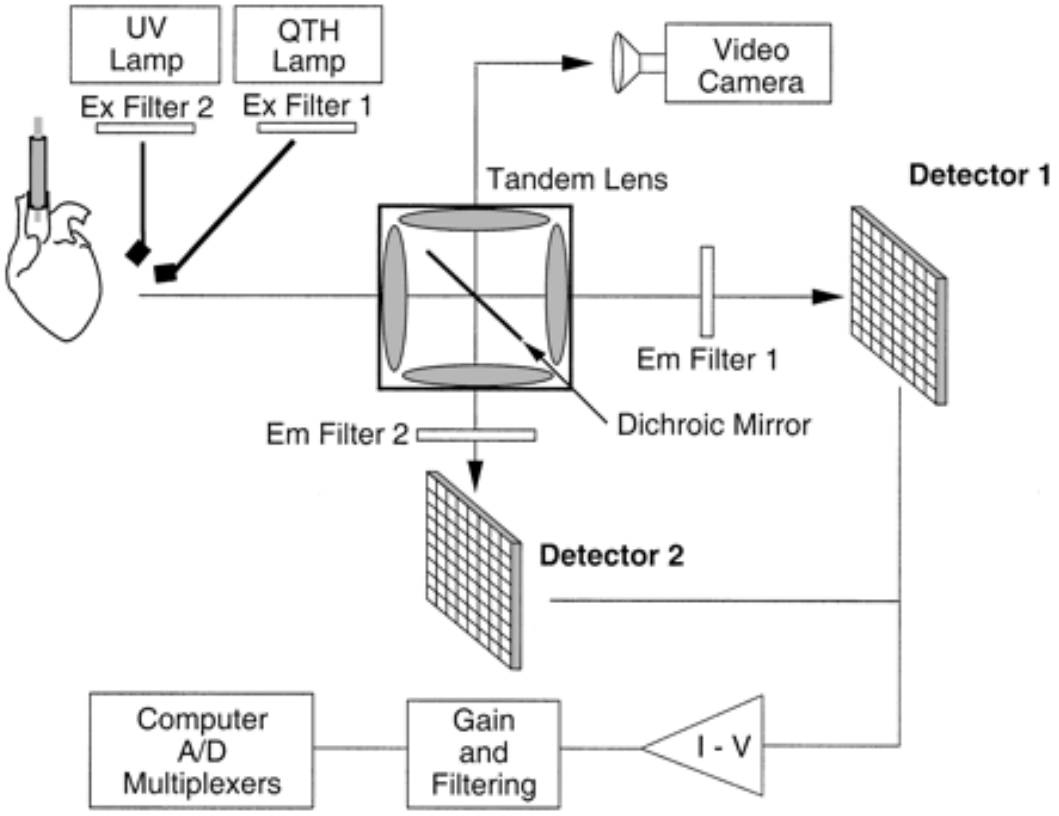

Fig. 1. Optical mapping system for simultaneously recording action potentials and calcium transients. Filtered [*Ex Filter 2* (365 ± 25 nm) and *Ex Filter 1* (515 ± 5 nm)] excitation light from a mercury arc lamp (250 W) and QTH lamp (180 W) is directed by liquid light guides to the same location on the preparation. Fluorescence is collected by a tandem lens system assembly consisting of 4 complex photographic lenses. A dichroic mirror passes fluorescence of longer wavelengths to an emission filter (*Em Filter 1* >695 nm) and detector array (*Detector 1*) and reflects fluorescence of shorter wavelengths to a second emission filter (*Em Filter 2*, 485 ± 5 nm) and detector array (*Detector 2*). A removable mirror inserted temporarily instead of the dichroic mirror redirects an image of the preparation to a charge coupled device videocamera. Signals from individual photodiodes are passed through an array of current-to-voltage (*I-V*) converters, amplified, filtered, and multiplexed to a 12-bit analog-to-digital (A/D) converter at 1,000 Hz per recording site. UV, ultraviolet.

The rats in the other four groups (each group containing about 15 rats) were fed with balanced diet, vata enhancing diet, pitta enhancing diet and kapha enhancing diet respectively for another three weeks and then using the above mentioned method were sacrificed and their Action potentials and Calcium transients were measured.

Vata enhancing diet (VED) included fresh uncooked vegetables with less oil content, cold and raw foods like dry cold cereal etc., raw sprouts, with bitter, pungent and astringent tastes.

Pitta enhancing diet (PED) included warm, spicy foods with pungent, salty and sour taste. More night shades were given.

Kapha enhancing diet (KED) included cold and cooked foods with lots of oils. Foods which were sweet were the chosen foods. Plenty of rie and wheat foods were chosen.

Experimental Protocol

A polytetrafluoroethylene-coated silver bipolar electrode with 1-mm interelectrode spacing was used to stimulate the anterior ventricular epicardial surface at twice diastolic threshold current. To ensure steady-state conditions, the preparation was paced at a constant baseline cycle length of 400 ms. The ECG, perfusion pressure, flow, and temperature were checked continuously throughout each experiment to monitor steady-state conditions.

To determine the amount of error caused by spectral overlap of di-4-ANEPPS and indo 1, two protocols were performed in separate experiments.

Protocol A. Hearts were first perfused with indo 1. The change in fluorescence emission was measured at >695 nm (i.e., emission filter normally used for di-4-ANEPPS) using 515 ± 5 and 365 ± 25 nm excitation, in the presence of indo 1 alone. The change in fluorescence intensity measured at >695 nm in the absence of di-4-ANEPPS is a direct measure of the error due to spectral overlap of indo 1 during measurement of action potentials [voltage potential (V_m) error]. Then the change in fluorescence was measured at 485 ± 5 nm using 365 ± 25 and 515 ± 5 nm excitation to measure intracellular calcium transients with no error due to spectral overlap of di-4-ANEPPS. Finally, hearts were loaded with di-4-ANEPPS, and with both indicators present, action potentials (V_m) and calcium transients (Ca^{2+}) were recorded simultaneously.

Protocol B. Hearts were first perfused with di-4-ANEPPS. The change in fluorescence emission was measured at 485 ± 5 nm (i.e., emission filter normally used for indo 1) using 515 ± 5 and 365 ± 25 nm excitation, in the presence of di-4-ANEPPS alone. The change in fluorescence intensity measured at 485 ± 5 nm in the absence of indo 1 is a direct measure of the error due to spectral overlap of di-4-ANEPPS during measurement of calcium transients (Ca^{2+} error). Then the change in fluorescence was measured at >695 nm using 365 ± 25 and 515 ± 5 nm excitation to measure action potentials with no error due to spectral overlap of indo 1. Finally, hearts were loaded with indo 1, and with both indicators present, action potentials (V_m) and calcium transients (Ca^{2+}) were recorded simultaneously.

Data Analysis

V_m and Ca^{2+} transients recorded simultaneously and error signals (i.e., V_m error and Ca^{2+} error) were recorded from all 256 mapping sites. To quantify signal magnitude, the

maximum change in fluorescence intensity corresponding to the maximum change in fluorescence during the upstroke of the action potential or the upstroke of the calcium transient (i.e., peak-to-peak amplitude) was calculated for every signal including error signals. Because excitation light and dye distribution are not uniform across the mapping field, V_m and Ca^{2+} error were calculated as a percent error, where peak-to-peak amplitude of V_m error and Ca^{2+} error signals were normalized to the peak-to-peak amplitude of V_m and Ca^{2+} measured in the presence of di-4-ANEPPS and indo 1 at each site

$$\%\,V_m\,\text{error} = (V_m\,\text{error}/[V_m - V_m\,\text{error}]) \times 100\% \quad (1)$$

for *protocol A* and

$$\%\,Ca^{2+}\,\text{error} = (Ca^{2+}\,\text{error}/[Ca^{2+} - Ca^{2+}\,\text{error}]) \times 100\% \quad (2)$$

for *protocol B*.

It is important to note that V_m and Ca^{2+} recordings were made with both indicators present. For example, V_m consisted of fluorescence due to di-4-ANEPPS and an error signal due to indo 1 (i.e., V_m error signal). Therefore, V_m error amplitude was subtracted from V_m amplitude in the denominator (*Eq. 1*) so that V_m error was determined as a percentage of fluorescence associated with a "pure" action potential.

The rise times of all optical action potential and calcium transient upstrokes were calculated as the time required for fluorescence to change from 10% to 90% of maximum. Depolarization times were calculated for all action potential recordings and defined as the time from stimulation to maximum positive derivative of the action potential upstroke (i.e., dV/dt_{max}). The onset of the calcium transient was calculated at all sites and defined as the time from stimulation to when fluorescence increased 25% above minimum diastolic level. Levels of significance were determined using a Student's *t*-test, where $P < 0.05$ was considered statistically significant.

RESULTS

Emission Spectra of Indo 1 and Di-4-ANEPPS

Figure 2 shows the emission spectra of indo 1 (excitation at 365 nm) and di-4-ANEPPS (excitation at 515 nm) measured in a representative experiment. Spectra were normalized to their peak fluorescence intensities. On the basis of the emission spectra, filters were chosen to minimize spectral overlap without significantly sacrificing signal strength. Superimposed on the emission spectrum of indo 1 is the normalized transmittance characteristics (as measured by the manufacturer) of the interference filter (shaded gray) chosen to measure calcium transients (Ca^{2+} emission filter, 485 ± 5 nm). To minimize contribution from di-4-ANEPPS, a filter with a narrow bandwidth and sharp cutoff wavelength was chosen near the peak emission of indo 1 (480 ± 3 nm, $n = 2$). Superimposed on the emission spectrum of di-4-ANEPPS are the normalized

transmittance characteristics (as measured by the manufacturer) of the long-pass filter chosen to measure action potentials (V_m emission filter, >695 nm). To minimize contribution from indo 1, a filter with a cutoff wavelength much greater than the emission spectra of indo 1 was chosen (V_m emission filter, >695 nm). As a consequence, the cutoff wavelength was significantly greater than the peak emission wavelength of di-4-ANEPPS (636 ± 2 nm, $n = 2$), which could significantly reduce the magnitude of action potential recordings.

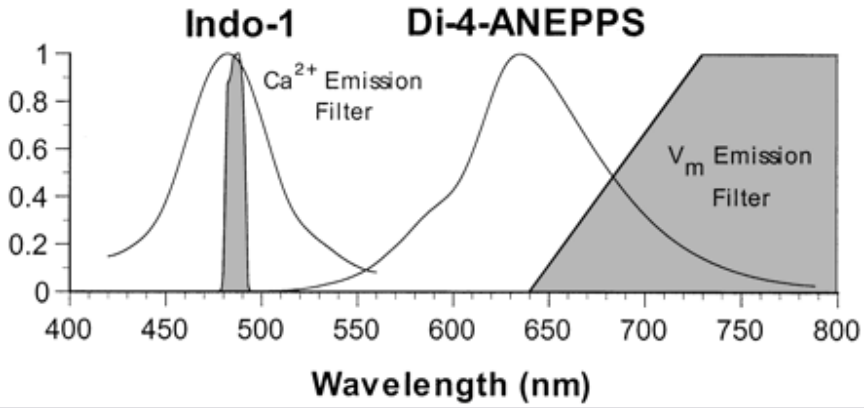

Fig. 2. Normalized transmittance characteristics of emission filters (gray area) selected for indo 1 (Ca^{2+} emission filter, 485 ± 5 nm) and di-4-ANEPPS [membrane potential (V_m) emission filter, >695 nm] superimposed on normalized emission spectra (solid lines) of indo 1 (excitation 365 nm) and di-4-ANEPPS (excitation 515 nm). On the basis of the emission spectra, filters were chosen to minimize spectral overlap and maximize signal strength.

On the basis of the spectra measured, the maximum error due to spectral overlap was expected to be minimal; however, because the absolute magnitude of the emission spectra was not taken into account, it is possible that the error due to overlap may be greater than predicted by the normalized spectra. In addition, with the use of the chosen filters, the magnitude of calcium transients and action potentials may be too small and, thus, significantly reduce signal fidelity. It is also possible that fluoresced light originating off the central optical axis does not strike the interference filter (Ca^{2+} filter) normal to its surface. This, theoretically, reduces the central wavelength of the interference filter by several nanometers and, thus, slightly increases the separation between Ca^{2+} and V_m filters. Therefore, a direct measurement of the error due to spectral overlap and the signal magnitude of action potentials and calcium transients over the entire mapping field was required.

Error Due to Spectral Overlap of Di-4-ANEPPS and Indo 1

To quantify the error due to spectral overlap of di-4-ANEPPS and indo 1, two separate experimental protocols were followed (*protocols A* and *B*). A representative example of fluorescence measurements made at a single recording site during each experimental

protocol is shown in Fig. 3. In *protocol A* (Fig. 3*A*), fluorescence change was first measured at >695 nm in the presence of indo 1 alone (Fig. 3*A, top trace*) with both excitation lights on. The change in fluorescence intensity represents the error due to spectral overlap of indo 1 during measurement of transmembrane potential (i.e., V_m error). Although difficult to see, the morphology of the V_m error signal is that of a calcium transient where fluorescence decreases on excitation, as expected with indo 1 emission at >695 nm. Fluorescence change was then measured again at >695 nm, but in the presence of indo 1 and di-4-ANEPPS, and is shown plotted on the same scale (Fig. 3*A, bottom trace*). As with fluorescence due to indo 1, fluorescence due to di-4-ANEPPS at >695 nm decreased on excitation (i.e., depolarization). In this case, the total change in fluorescence intensity (i.e., V_m) included fluorescence changes due to di-4-ANEPPS and indo 1; however, V_m error relative to the change in fluorescence due to di-4-ANEPPS, calculated using *Eq. 1*, was very small (0.84%) and was not visually apparent on the action potential recording.

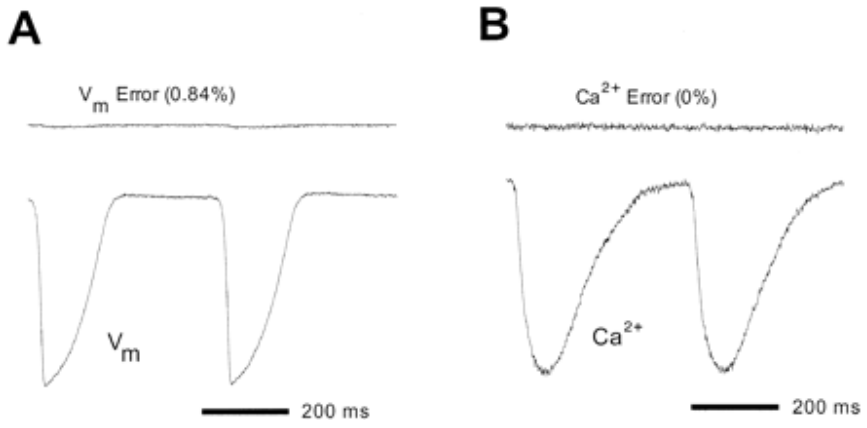

Fig. 3. *A*: *protocol A*. Change in fluorescence measured from a single recording site at >695 nm with both excitation sources on in the presence of indo 1 alone (*top trace,* V_m error) and in the presence of di-4-ANEPPS and indo 1 (*bottom trace,* V_m) drawn on the same scale. The error signal is small compared with the total change in fluorescence (0.84%). *B*: *protocol B*. Change in fluorescence measured from a single recording site at 485 ± 5 nm with both excitation sources on in the presence of di-4-ANEPPS alone (*top trace*, Ca^{2+} error) and in the presence of indo 1 and di-4-ANEPPS (*bottom trace*, Ca^{2+}) drawn on the same scale. The error signal was smaller than the detectable range of our system.

In *protocol B*, fluorescence change was first measured at 485 ± 5 nm in the presence of di-4-ANEPPS alone (Fig. 3*B, top trace*) with both excitation lights on. The change in fluorescence intensity represents a direct measurement of the error due to spectral overlap of di-4-ANEPPS emission during measurement of intracellular calcium (i.e., Ca^{2+} error). The Ca^{2+} error signal was undetectable with our system resolution. Fluorescence change was measured again using the same Ca^{2+} filters with both light sources on and in the

presence of both di-4-ANEPPS and indo 1 and is shown plotted on the same scale (Fig. 3*B, bottom trace*). At this emission wavelength (485 ± 5 nm), fluorescence due to indo 1 decreased on excitation. In this case, the total change in fluorescence intensity (i.e., Ca^{2+}) consisted of fluorescence only from indo 1.

We determined that the percent V_m error and Ca^{2+} error were small throughout the entire mapping field. The percent V_m error calculated using *Eq. 1* over the entire mapping field from a representative experiment is shown in Fig. 4. The average percent V_m error was extremely small (0.92 ± 0.94%) and at many sites undetectable. However, the percent V_m error was as high as 4%. In contrast, the percent Ca^{2+} error was undetectable with the resolution of our recording system across the entire mapping field (not shown). V_m error was greater than Ca^{2+} error, indicating greater spectral overlap between di-4-ANEPPS and indo 1 at >695 nm than at 485 ± 5 nm. Nevertheless, as shown in Table 1, the average percent error due to spectral overlap was extremely small over all experiments.

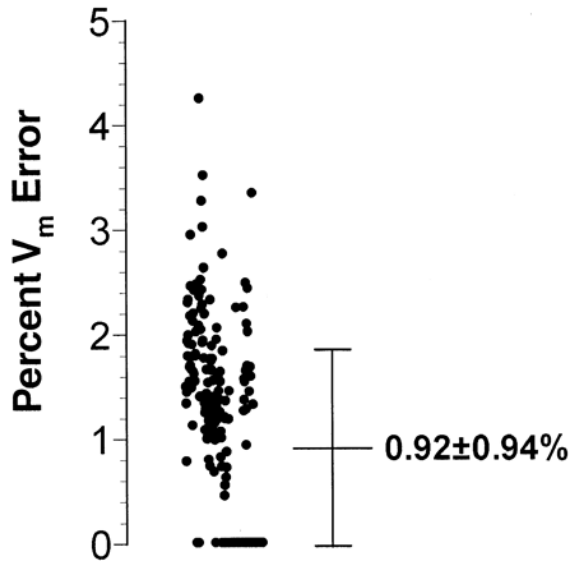

Fig. 4. Percent V_m error over the entire mapping field from a representative experiment. ●, Individual recording sites in the mapping field array. Horizontal bars, mean and SD. Over the entire mapping field, the error due to spectral overlap is small (0.92 ± 0.94%). In many cases, the error was below the resolution of our mapping system (i.e., 0%).

Table 1. Summary data for percent V_m error and percent Ca^{2+} error

Table 1. Summary data for percent V_m error and percent Ca^{2+} error

Expt. No.	% V_m Error (*protocol A*)	% Ca^{2+} Error (*protocol B*)
1	2.9	
2	0.9	
3	1.4	
4		0.0
5		0.0
6		0.0
Mean ± SD	1.7 ± 1.0%	0.0%

Data demonstrate the effect of spectral overlap between indo 1 and di-4-ANEPPS. The value shown for each individual experiment is the mean value for all 256 recording sites. For *protocol A,* percent membrane potential (V_m) error was very small for all experiments; for *protocol B,* percent Ca^{2+} error was always less than the detectable range of our recording system.

Action Potentials and Calcium Transients Measured Simultaneously

After measurement of the error due to spectral overlap of indo 1 and di-4-ANEPPS, calcium transients and action potentials were recorded simultaneously during each experiment ($n = 6$). A representative example of an action potential and calcium transient recorded simultaneously from the same site in the presence of indo 1 and di-4-ANEPPS is shown in Fig. 5. In the action potential recording (Fig. 5, *top*), a rapid upstroke and all phases of the action potential are clearly visible with no apparent artifact due to spectral overlap of indo 1 (V_m error). The calcium transient recorded from the same site (Fig. 5, *bottom*) also shows no noticeable error due to spectral overlap of di-4-ANEPPS. The initial rapid increase in intracellular calcium followed the upstroke of the action potential by 7 ms in this example, and the decrease in intracellular calcium to minimum diastolic levels occurred well beyond the repolarization phase of the action potential. The average rise time of optical action potential upstrokes for all experiments was 7.9 ± 2.9 and 8.4 ± 3.0 ms in the absence and presence, respectively, of indo 1 (not significant). Similarly, the average rise time of calcium transient upstrokes in all experiments was 14.4 ± 2.2 and 15.9 ± 1.0 ms in the absence and presence, respectively, of di-4-ANEPPS (not significant). These data indicate that the extremely small error due to spectral overlap of indo 1 and di-4-ANEPPS does not influence measurements when the change in fluorescence and, thus, the error due to overlap are expected to be greatest (i.e., during the action potential and calcium transient upstroke).

Fig. 5. A representative example of an action potential and calcium transient recorded simultaneously from the same site after perfusion of the heart with both indo 1 and di-4-ANEPPS.

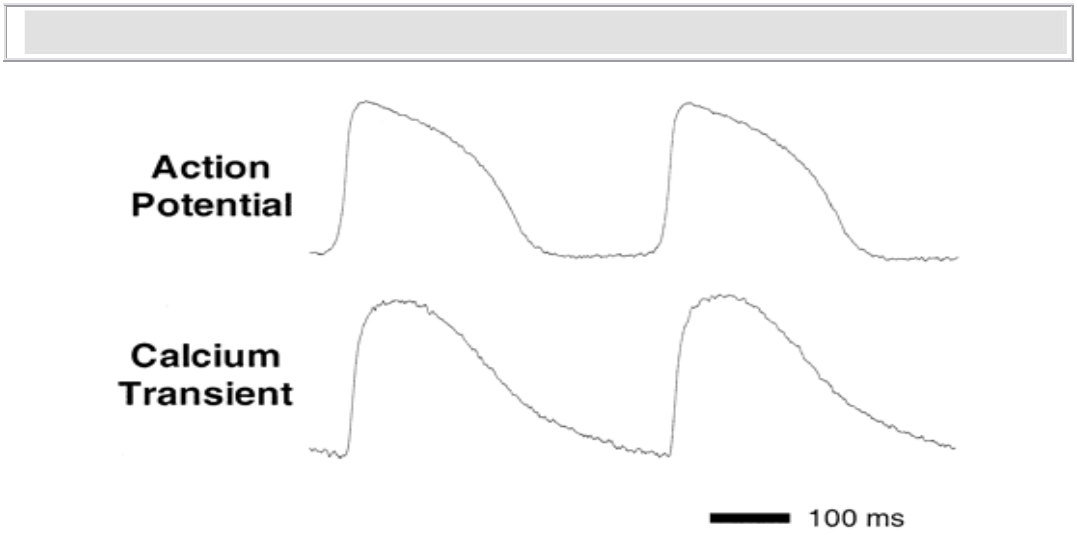

Action potentials and calcium transients were recorded simultaneously from all 256 sites within the mapping field. Isochrone maps of depolarization time and the time of calcium transient onset relative to the time of stimulation are shown in Fig. 6. The spread of depolarization (Fig. 6*A*) indicates anisotropic propagation from the site of stimulation (pacing symbol) with an average conduction velocity of 54 cm/s along the fast axis of propagation. Calcium transients were also recorded from the same 256 recording sites, and the time of calcium transient onset was calculated for each site (Fig. 6*B*). The spatial pattern of the calcium transient onset was also anisotropic and, as expected, closely mirrored that of electrical activation. The site of earliest depolarization occurred at 5 ms, followed by the onset of the calcium transient at 10 ms. The calcium transient onset and depolarization times were distributed such that the action potential always preceded the onset of the calcium transient by, on average, 7.8 ± 2.8 ms over the entire mapping field. These data indicate negligible error due to spectral overlap of indo 1 and di-4-ANEPPS over the entire mapping field.

Fig. 6. Contour maps of depolarization time (*A*) and the time of calcium transient onset (*B*) calculated from action potentials and calcium transients recorded simultaneously from 256 sites on the epicardial surface of the intact guinea pig heart. The contour legend represents both panels, where each contour interval indicates 5 ms and the fiducial point (i.e., 0 ms) corresponds to the time of stimulation (pacing symbol). As expected, the pattern of depolarization is mirrored by, after a slight delay, the pattern of calcium transient onset.

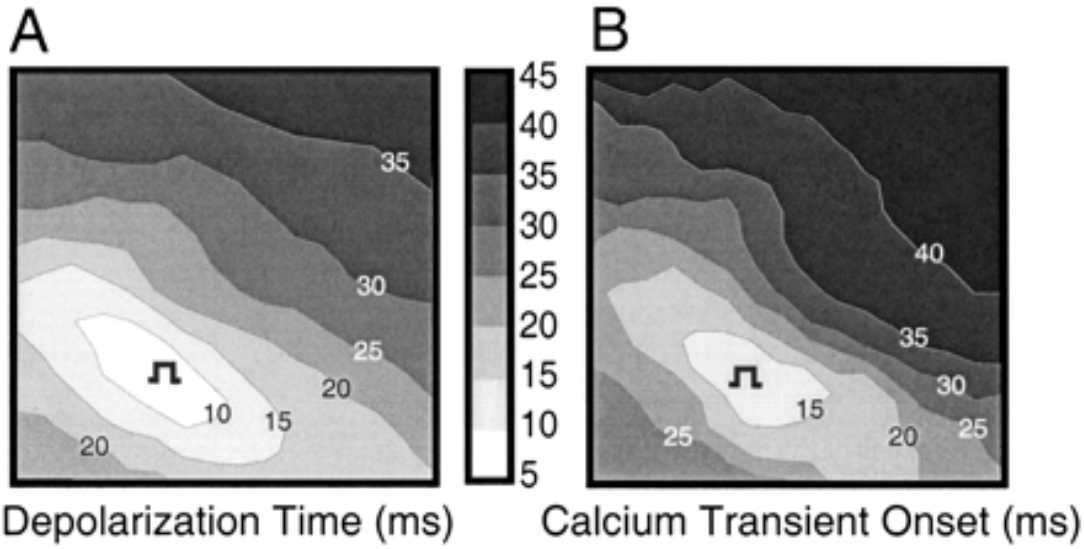

Table 2

	Experimental values				
	Control group 1	**Control group 2**	**VED fed rats**	**PED fed rats**	**KED fed rats**
Resting Potential V, mV	**- 84.5 ± 3.00**	**- 85.67 ± 3.00**	**- 70.45 ± 4.5**	**- 90 ± 3.5**	**- 108.78 ± 3.5**

As seen from the table the control groups of rats had nearly the same resting potential. The VHD fed rats had a resting potential which were very near to the threshold potential which in all rats measured around -65mV ± 2.5. On the contrary the KED fed rats had lower resting potentials than even the PED fed rats making their cells more stable.

.

DISCUSSION

We have observed the effects of the various diets as described in the Ayurvedic texts does have impact on the resting potentials of the heart cells. Basing on our results we state that the cells resting potentials vary between -70 and -110mV approximately (Table 2). The cells in the VED fed rats have a resting potential which is very near to the

threshold potential. It means that the cells would require only a smaller stimulus to excite an action potential. On the contrary the KED cells appear to be more stable requiring a stronger stimulus to generate action potential. We have described and validated a new technique based on optical mapping that is capable of measuring calcium transients and action potentials simultaneously from the intact heart. Two fluorescent indicators were chosen that have previously been used extensively to measure intracellular calcium (indo 1) and transmembrane potential (di-4-ANEPPS). We demonstrate that the error due to spectral overlap of indo 1 and di-4-ANEPPS is very small. As a result, intracellular calcium transients and action potentials can be mapped simultaneously with high signal fidelity from the same heart with negligible error. This technique may provide significant insight into the cellular mechanisms of arrhythmias associated with abnormal intracellular calcium handling.

To simultaneously measure intracellular calcium and transmembrane potential in the same heart, two fluorescent indicators were used. The indicators chosen in the present study were di-4-ANEPPS (23) for sensing transmembrane potential and indo 1 (12) for sensing free intracellular calcium concentration. These particular indicators were chosen because *1*) both have been well characterized and independently accepted as standard techniques and *2*) the wavelengths of peak emission are significantly separated, minimizing spectral overlap. Figure 2 illustrates this point. Both spectra correspond to fluorescence emission at resting membrane potential (di-4-ANEPPS) and low intracellular calcium levels (indo 1). The gray areas in Fig. 2 indicate the wavelengths at which calcium transients (Ca^{2+} filter) and action potentials (V_m filter) were measured in the present study. As indicated in Fig. 2, when fluorescence is measured using Ca^{2+} or V_m filters, fluorescence originates from both indicators; however, the contribution of one is much larger than that of the other. For example, the change in fluorescence intensity at 485 ± 5 nm (i.e., area under both spectral curves bounded by 485 ± 5 nm) is mostly due to indo 1; however, a small amount of fluorescence change may arise from di-4-ANEPPS and is what we called Ca^{2+} error. Likewise, fluorescence changes at >695 nm arise mostly from di-4-ANEPPS with a small contribution from indo 1 (V_m error). If emission spectra or optical filters were closer in wavelength, significant overlap would occur, resulting in a composite signal consisting of significant fluorescence from di-4-ANEPPS and indo 1.

With a judicious selection of optical filters, we found that the error due to spectral overlap of indo 1 and di-4-ANEPPS was sufficiently small, such that calcium transients and action potentials could be measured simultaneously from the intact heart with negligible error. We found that V_m error due to fluorescence of indo 1 was, on average, extremely small ($1.7 \pm 1.0\%$) and at many sites zero. The variability in error across the mapping field could be explained by an unequal distribution of relative intensity of excitation light at 365 and 514 nm and/or relative dye concentration. Indeed, error variability due to differences in relative fluorescence intensity of fluo 3/4 and di-4-ANEPPS was analyzed in a study by Johnson et al. (14) and was similar in magnitude to that measured in the present study. The Ca^{2+} error due to fluorescence change of di-4-ANEPPS was so small that it was undetectable with the resolution of our mapping system. On the basis of the emission spectra and the transmission characteristics of the optical filter chosen, this is not a surprise. It is possible, on the basis of biological and dye loading variability, that the contribution of one dye may become much stronger than that of the other. In such a case, the error due to overlap might become significant. It may be

possible to compensate for such differences in dye loading by adjusting excitation light intensity. For example, if action potentials are significantly larger than calcium transients, then the excitation light used to maximally excite di-4-ANEPPS can be reduced. However, reducing excitation intensity would also lower the signal amplitude of the action potentials and, thus, reduce signal fidelity. In the present study, to achieve high signal fidelity, excitation intensity was maintained at levels normally used for measuring action potentials and calcium transients independently. Finally, our experimental protocols to measure error due to spectral overlap were not designed to test the possibility of indo 1 emission exciting di-4-ANEPPS. Although this is theoretically possible, it is unlikely to affect our results, because the change in fluorescence intensity associated with indo 1 is much smaller than the amount of excitation light required to generate significant fluorescence of di-4-ANEPPS. Experiments specifically designed to test this possibility support our conclusion (unpublished observation).

The error due to spectral overlap of indo 1 and di-4-ANEPPS was negligible, making it possible to map with confidence calcium transients and action potentials from the intact heart with high resolution. The calcium transient and action potential shown in Fig. 5 demonstrate a rapid rise in intracellular calcium several milliseconds after the upstroke of the action potential. This result is expected on the basis of the theory of calcium-induced calcium release (8). The decline of intracellular calcium is much slower, extending beyond the repolarization phase of the action potential when transmembrane potential is at rest. The rise time of calcium transients measured in this study is comparable to that measured previously (6). Moreover, the rise times of the calcium transients and optical action potentials were unaffected by the presence of both di-4-ANEPPS and indo 1. At all 256 mapping sites, action potentials and calcium transients exhibited a close spatial relationship. The contour maps shown in Fig. 6 demonstrate the pattern of depolarization time and time of calcium transient onset. Throughout the entire mapping field, action potential propagation (Fig. 6*A*), after a delay, is mirrored by the calcium transient onset (Fig. 6*B*). These data provide further evidence that the error due to spectral overlap of indo 1 and di-4-ANEPPS is negligible and that this technique can be used to map with high resolution calcium transients and action potential simultaneously in the intact heart. In preliminary studies using a similar technique, it was possible to investigate intracellular calcium handling and repolarization alternans (19) and to examine the relationship between action potentials and calcium transients during reentrant excitation (20).

Intracellular calcium and transmembrane potential have been measured previously in the same heart (4, 7, 21). However, in these studies, recordings could be made from only one site at a time. This limitation may hinder the investigation of certain arrhythmia mechanisms. Recently, using an approach slightly different from that used in the present study, Fast and Ideker. (9) developed a technique for mapping action potentials and calcium transients in myocyte cultures. With the use of the voltage-sensitive dye RH-237 and the calcium-sensitive dye fluo 3, action potentials and calcium transients were recorded with negligible error. In the present study, we measured changes in fluorescence intensity of indo 1 and not absolute intracellular free calcium levels. Nevertheless, indo 1, unlike fluo 3, has a second emission peak that occurs at ~405 nm, corresponding to the bound form of indo 1. This peak could be used to further reduce spectral overlap and,

more importantly, could also be used to measure actual intracellular calcium levels throughout the heart using standard ratiometric imaging techniques (34).

Clinical Implications

The Vata cells thus are very susceptible to extremely low stimuli and are capable of exciting action potentials even with low stimuli. From this it may be hypothesized that if say there is an accumulation of more Vata in the Immune cells then it may result in Hypersensitivity reaction like allergies and asthma etc., If the same is applied to nerve cells the vata nerve cell may result in sleep disorders and so on. The Pitta cells are stable and represent the normal metabolic functioning of the body. The Kapha cells are more stable than the Pitta cells and their excitation requires stronger stimuli. If kapha increases in say for example, the Immune cells again the immune response occurs only to a stronger bacterial or allergic stimulus and so hypersensitivity reactions do not occur in such individuals. There is also a possibility of a symbiotic environment in such individuals. Here kapha should not be confused with a hefty person. Vata, Pittaand Kapha are only various Action potential states of cell. In the course of this experiment we also have concluded the following:

Because intracellular calcium plays a critically important role in the electrophysiology of the heart, there are several important clinical implications of abnormal intracellular calcium handling. T wave alternans, a known predictor of sudden cardiac death (31), has been mechanistically linked to repolarization alternans and the initiation of ventricular fibrillation (28) and torsade de pointes (33). It has been suggested that intracellular calcium handling plays a significant role in the cellular mechanisms of repolarization alternans (17, 32, 33); however, a causal relationship has yet to be determined. We have shown, in a preliminary study, that in the intact heart, spatial heterogeneity of repolarization alternans is closely mirrored by spatial heterogeneity of calcium transient alternans (19). Heart failure is another significant clinical paradigm that is associated with a high incidence of sudden cardiac death and the occurrence of ventricular (5) and atrial (25) arrhythmias. Intracellular calcium homeostasis is believed to be significantly altered in failing hearts due to, in part, upregulation of Na^{+}/Ca^{2+} exchanger (35) and impaired uptake of calcium by the sarcoplasmic reticulum (13). Such alterations of intracellular calcium handling may lead to calcium overload and, in turn, the occurrence of delayed afterdepolarizations. Delayed afterdepolarizations have been associated with triggered arrhythmias in failing hearts (36). Undoubtedly, the ability to map intracellular calcium and transmembrane potential simultaneously in the intact heart will provide new and important information concerning the cellular mechanisms of arrhythmias associated with abnormal intracellular calcium handling.

ACKNOWLEDGEMENTS

This work was supported by a grant from Sai Ganga Panacea LLC, a Delaware corporation, whose Chairmand CEO is DR. Ravishankar POlisetty.

REFERENCES

1. **Blinks, JR, Wier WG, Hess P, and Prendergast FG.** Measurement of Ca^{2+} concentrations in living cells. *Prog Biophys Mol Biol* 40: 1-114, 1982.

2. **Boyett, MR, Harrison SM, Janvier NC, McMorn SO, Owen JM, and Shui Z.** A list of vertebrate cardiac ionic currents. Nomenclature, properties, function and cloned equivalents. *Cardiovasc Res* 32: 455-481, 1996.

3. **Brandes, R, Figueredo V, Camacho S, Baker A, and Weiner M.** Quantitation of cytosolic [Ca^{2+}] in whole perfused rat hearts using indo 1 fluorometry. *Biophys J* 65: 1973-1982, .

4. **Burdyga, T, and Wray S.** Simultaneous measurements of electrical activity, intracellular [Ca^{2+}] and force in intact smooth muscle. *Pflügers Arch* 435: 182-184, 1997.

5. **Chakko, CS, and Gheorghiade M.** Ventricular arrhythmias in severe heart failure: incidence, significance, and effectiveness of antiarrhythmic therapy. *Am Heart J* 109: 497-504, 1985.

6. **Cleemann, L, and Morad M.** Role of Ca^{2+} channel in cardiac excitation-contraction coupling in the rat: evidence from Ca^{2+} transients and contraction. *J Physiol (Lond)* 432: 283-312, 199.

7. **Clusin, W, Han J, and Quan Y.** Simultaneous recordings of calcium transients and action potentials from small regions of the perfused rabbit heart. *PACE* 22: 834, 1999.

8. **Fabiato, A.** Time and calcium dependence of activation and inactivation of calcium-induced release of calcium from the sarcoplasmic reticulum of a skinned canine cardiac Purkinje cell. *J Gen Physiol* 85: 247-89, 1985.

9. **Fast, VG, and Ideker RE.** Simultaneous optical mapping of transmembrane potential and intracellular calcium in myocyte cultures. *J Cardiovasc Electrophysiol* 11: 547-556, 2000.

10. **Girouard, SD, Pastore JM, Laurita KR, Gregory KW, and Rosenbaum DS.** Optical mapping in a new guinea pig model of ventricular tachycardia reveals mechanisms for multiple wavelengths in a single reentrant circuit. *Circulation* 93: 603-613, 1996.

11. **Gray, RA, Jalife J, Panfilov AV, Baxter WT, Cabo C, Davidenko JM, and Pertsov AM.** Mechanisms of cardiac fibrillation. *Science* 270: 1222-1223, 1995.

12. **Grynkiewicz, G, Poenie M, and Tsien RY.** A new generation of Ca^{2+} indicators with greatly improved fluorescence properties. *J Biol Chem* 260: 3440-3450, 1985.

13. **Gwathmey, JK, Copelas L, MacKinnon R, Schoen FJ, Feldman MD, Grossman W, and Morgan JP.** Abnormal intracellular calcium handling in myocardium from

patients with end-stage heart failure. *Circ Res* 61: 70-76, 1987.

14. **Johnson, PL, Smith W, Baynham TC, and Knisley SB.** Errors caused by combination of di-4 ANEPPS and fluo3/4 for simultaneous measurements of transmembrane potentials and intracellular calcium. *Ann Biomed Eng* 27: 563-571, 1999.

15. **Juang, G, Ohler A, Wu R, Burysek M, O'Rourke B, and Tomaselli GF.** Regional changes in calcium handling proteins in canine pacing tachycardia heart failure (Abstract). *Circulation* 102: II-92, 2000.

16. **Knisley, SB.** Mapping intracellular calcium in rabbit hearts with fluo 3. In: *Proc 17th Annu Int Conf IEEE Eng Med Biol Soc*, 1995, p. 455-456.

17. **Kobayashi, Y, Peters W, Khan SS, Mandel WJ, and Karagueuzian HS.** Cellular mechanisms of differential action potential duration restitution in canine ventricular muscle cells during single versus double premature stimuli. *Circulation* 86: 955-967, 1992.

18. **Laurita, KR, Girouard SD, and Rosenbaum DS.** Modulation of ventricular repolarization by a premature stimulus: role of epicardial dispersion of repolarization kinetics demonstrated by optical mapping of the intact guinea pig heart. *Circ Res* 79: 493-503, 1996

19. **Laurita, KR, Singal A, Pastore JM, and Rosenbaum DS.** Spatial heterogeneity of calcium transients may explain action potential dispersion during T-wave alternans (Abstract). *Circulation* 98: I-187, 1998.

20. **Laurita, KR, Singal A, and Rosenbaum DS.** High-resolution optical mapping of intracellular calcium and transmembrane potential during reentry. *Pacing Clin Electrophysiol* 22: 702, 1999.

21. **Lee, HC, Mohabir R, Smith N, Franz MR, and Clusin WT.** Effect of ischemia on calcium-dependent fluorescence transients in rabbit hearts containing indo-1: correlation with monophasic action potentials and contraction. *Circulation* 78: 1047-1059, 1988.

22. **Libbus, I, Eloff BC, Girouard SD, and Rosenbaum DS.** Advantages and limitations of a tandem lens design in high-resolution optical imaging (Abstract). *Ann Biomed Eng* 26: S-19, 1998.

23. **Loew, LM, Cohen LB, Dix J, Fluhler EN, Montana V, Salama G, and Jian-Young W.** A naphthyl analog of the aminostyryl pyridinium class of potentiometric membrane dyes shows consistent sensitivity in a variety of tissue, cell, and model membrane preparations. *J Membr Biol* 130: 1-10, 1992.

24. **McIntosh, MA, Cobbe SM, and Smith GL.** Heterogeneous changes in action potential and intracellular Ca^{2+} in left ventricular myocyte subtypes from rabbits with heart failure. *Cardiovasc Res* 45: 397-409, 2000.

25. **Middlekauff, HR, Stevenson WG, and Stevenson LW.** Prognostic significance of atrial fibrillation in advanced heart failure. A study of 390 patients. *Circulation* 84: 40-48, 1991.

26. **Mohabir, R, Clusin TW, and Lee HC.** Intracellular calcium alternans and the genesis of ischemic ventricular fibrillation. In: *Cardiac Electrophysiology: From Cell to Bedside*, edited by Zipes DP, and Jalife J.. Philadelphia, PA: Saunders, 1990, p. 448-456.

27. **Morad, M, and Salama G.** Optical probes of membrane potential in heart muscle. *J Physiol (Lond)* 292: 267-295, 1979.

28. **Pastore, JM, Girouard SD, Laurita KR, Akar FG, and Rosenbaum DS.** Mechanism linking T-wave alternans to the genesis of cardiac fibrillation. *Circulation* 99: 1385-1394, 1999.

29. **Pogwizd, SM.** Nonreentrant mechanisms underlying spontaneous ventricular arrhythmias in a model of nonischemic heart failure in rabbits. *Circulation* 92: 1034-1048, 1995.

30. **Ratzlaff, EH, and Grinvald A.** A tandem-lens epifluorescence macroscope: hundred-fold brightness advantage for wide-field imaging. *J Neurosci Methods* 36: 127-137, 1991.

31. **Rosenbaum, DS, Jackson LE, Smith JM, Garan H, Ruskin JN, and Cohen RJ.** Electrical alternans and vulnerability to ventricular arrhythmias. *N Engl J Med* 330: 235-241, 1994.

32. **Rubenstein, DS, and Lipsius SL.** Premature beats elicit a phase reversal of mechanoelectrical alternans in cat ventricular myocytes: a possible mechanism for reentrant arrhythmias. *Circulation* 91: 201-214, 1995.

33. **Shimizu, W, and Antzelevitch C.** Cellular and ionic basis for T-wave alternans under long-QT conditions. *Circulation* 99: 1499-1507, 1999.

34. **Sipido, KR, and Callewaert G.** How to measure intracellular [Ca^{2+}] in single cardiac cells with fura-2 or indo-1. *Cardiovasc Res* 29: 717-726, 1995.

35. **Studer, R, Reinecke H, Vetter R, Holtz J, and Drexler H.** Expression and function of the cardiac Na^{+}/Ca^{2+} exchanger in postnatal development of the rat, in experimental-induced cardiac hypertrophy and in the failing human heart. *Basic Res Cardiol* 92 *Suppl*1: 53-58, 1997.

36. **Vermeulen, JT, McGuire MA, Opthof T, Coronel R, de Bakker JM, Klopping C, and Janse MJ.** Triggered activity and automaticity in ventricular trabeculae of failing human and rabbit hearts. *Cardiovasc Res* 28: 1547-1554, 1994.

37. **Vermeulen, JT, McGuire MA, Opthof T, Coronel R, de Bakker JMT, Klöpping C, and Janse MJ.** Triggered activity and automaticity in ventricular trabeculae of failing

human and rabbit hearts. *Cardiovasc Res* 28: 1547-1554, 1994.

38. **Witkowski, FX, Leon LJ, Penkoske PA, Giles WR, Spano ML, Ditto WL, and Winfree AT.** Spatiotemporal evolution of ventricular fibrillation. *Nature* 392: 78-82, 1998.

39. **Vagbhat's Astanga Hrdayam, Krishnadas Ayurveda Series Vol. 27;** Translated by Prof. K. R. Srikantha Murthy.